www.czasopisma.pan.pl PAN POLSKA AKADEMIA NAUK www.journals.pan.pl

Arch. Metall. Mater. **63** (2018), 4, 2081-2087

DOI: 10.24425/amm.2018.125146

A. CWUDZIŃSKI*#, B. GAJDA*, A. HUTNY*, J. JOWSA*

MATHEMATICAL AND PHYSICAL MODELING OF ALLOY BEHAVIOR FEEDING BY PULSE-STEP METHOD TO LIQUID STEEL IN ONE STRAND SLAB TUNDISH

The main purpose of the present work was to validate the numerical model for the pulse-step liquid steel alloying method using a physical simulator that enables the observation and recording of phenomena occurring during the continuous steel casting process. The facility under investigation was a single-nozzle tundish equipped with a dam. To physical trials the glass water model was made on a scale of 2:5. For the mathematical description of turbulence during liquid steel alloying process, the k-ε and k-ω models were employed in the simulations. Based on the computer simulations and physical trials carried out, alloy addition behaviour and mixing curves for different tundish alloy addition feeding positions were obtained. The change in the location of alloy addition feeding to the liquid steel had an effect on the process of alloy addition spread in the liquid steel bulk and on the mixing time.

Keywords: tundish, pulse-step alloying method, liquid steel, physical trials, numerical modeling

1. Introduction

Liquid steel casting technologies are the subject of studies by leading research centres worldwide [1-4]. At the continuous casting stage, alloying of liquid steel in the tundish or in the mould refers chiefly to the introduction of low-melting alloys or technical metals, including non-metallic inclusions modifiers that enable the correction of the composition of the steel or precipitates. Therefore, the efficiency of the steel alloying process will be determined by a hydrodynamic pattern forming in a given continuous steel casting machine. At the continuous steel casting stage, the liquid steel resides in the tundish much longer than in the mould, therefore the tundish seems to be a potentially easier facility, which could aid the technologies of feeding alloy additions to liquid steel. In the tundish working space, a characteristic hydrodynamic pattern forms, which is created by flowing liquid steel streams [5-12]. Individual liquid steel streams form as a result of interaction between the flowing liquid steel and the tundish walls or flow control devices (FCDs) installed in the tundish' interior. The shapes and geometries of tundishes are adapted to specific continuous steel casting machines, depending on the number and form of billets, blooms or slabs to be cast. Obviously, the more moulds are handled by a tundish, the more difficult is to attain uniform hydrodynamic conditions within the entire facility. In order to influence the hydrodynamics in tundishes, FCDs are installed to efficiently modify the liquid steel motion. Moreover, FCDs may either decelerate or accelerate the flow of liquid steel through the tundish. In addition, FCDs may have an effect on non-metallic phases in the form of non-metallic inclusions or tundish powder [13-16]. Also in the case of feeding an alloy addition to liquid steel, the chemical homogenization process will be determined by the liquid steel flow hydrodynamics and the alloy addition feed position [17-18]. Based on the computer simulations and physical trials carried out, alloy addition behaviour and mixing curves for different tundish alloy addition feeding positions were obtained.

2. Methodology of research

The facility under investigation was a single-nozzle tundish equipped with a dam. The dam protects the stopper rod against the shock wave flowing in from the pouring zone side during starting the casting sequence. The tundish is described in detail in study [19]. Considering a peculiar design of the investigated facility, four alloy addition feed locations were selected, which were situated within the tundish pouring zone. The selected alloy addition feed locations were meant to provide an optimal time of alloy addition residence in the tundish, which would allow the alloy addition to effectively spread within the liquid steel volume. The selected alloy addition feeding positions (AAFP) are indicated in Figure 1a. The figure illustrating the virtual tundish model indicates also three points at which the variation in alloy addition concentration in the liquid steel was monitored. Figure 1b shows a laboratory test stand with a glass tundish model. The model was made on a scale of 2:5. The

* CZESTOCHOWA UNIVERSITY OF TECHNOLOGY, FACULTY OF PRODUCTION ENGINEERING AND MATERIALS TECHNOLOGY, DEPARTMENT OF METALS EXTRACTION AND RECIRCULATION, 19 ARMII KRAJOWEJ AV., 42-200 CZESTOCHOWA, POLAND

Corresponding author: cwudzinski@wip.pcz.pl

linear scale of the model ensures geometric similarity to the real facility. Whereas, dynamic similarity is ensured by Froude criterion. In numerical simulations, the alloy addition was steel scrap with physicochemical properties identical to those of the steel grade being cast. In physical simulations, on the other hand, the medium representing liquid steel was water, while the alloy addition was simulated with a 2% NaCl solution. During the laboratory tests, change in NaCl concentration was recorded using conductometric sensors. In both cases i.e. numerical and physical simulations, the alloy addition would has a liquid form. This simplification was possible, because industrial experiments made previously had shown that, with an appropriately small size of alloy addition pieces, the duration of alloy addition dissolution in the liquid steel was short enough to not significantly disturb the macro-mixing process [20]. The research objective was to verify the correctness of the numerical model's assumptions and limitations in the form of boundary conditions for simulation of feeding an alloy addition to liquid steel by the pulse-step method (PSM) and to evaluate the consistence of the results obtained by computations with the process picture obtained from the physical simulator. The physical simulations were possible by additionally equipping the testing stand with a peristaltic pump to enable the precision feed of the alloy addition-simulating solution in a continuous manner. Computer simulations were performed using the software program Ansys-Fluent. For the mathematical description of alloy addition behavior in liquid steel, the species model was used. The computer simulations were carried out for isothermal conditions. A detailed description of the model and the physicochemical properties of the liquid steel is provided in study [20]. For the mathematical description of turbulence, the k-ε and k-ω models were employed in the simulations. The realizable k-ε turbulence model include an alternative formulation for the turbulent viscosity by considering vorticity fluctuation. While the standard k-ω turbulence model calculated turbulence motion of fluid by means of specific dissipation rate. Generally specific dissipation rate is defined as ratio of ε to k. At an initial liquid steel velocity of 1.31 m/s, in the case of the k-ε model, k and ε amounted to, respectively, 0.017161 m^2/s^2 and 0.064231 m^2/s^3. Whereas, in the case of the second turbulence model, ω was 50.38 1/s. In the case of the w parameter, the diameter of the steelmaking ladle's shroud was taken into consideration. Based on the mixing characteristics, the mixing time will be calculated. A reference level for calculating the mixing time required for achieving a chemical homogenisation level of 95% will be the alloy addition quantity recorded at the tundish outlet at the time of finishing the casting of the heat. The level of chemical homogenisation was determined using the following relationship:

$$C_{PSM} = \frac{(C_t - C_0)}{(C_f - C_0)} \cdot 100\% \tag{1}$$

where: C_f – final concentration of alloy at tundish outlet (wt%), C_{PSM} – dimensionless concentration of alloy for PSM, C_t – temporary concentration of alloy (wt%), C_0 – initial concentration of alloy (wt%).

Based on the mixing curves, the dimensionless mixing time (DMT) was calculated. The DMT is defined as the time, after which the minimum required liquid steel chemical homogenisation level is maintained, which should amount to at least 95%. A reference level for calculating the mixing time required for achieving a 95% chemical homogenization level was the alloy addition quantity recorded at the tundish outlet at the finish of heat casting. The time interval was expressed by DMT defined by the ratio of the actual time to the average time. The average time for the tundish under examination and numerical simulations was 735 seconds.

3. Preliminary research

At the first stage of the computer simulations, different locations of the monitoring point of alloy addition concentration

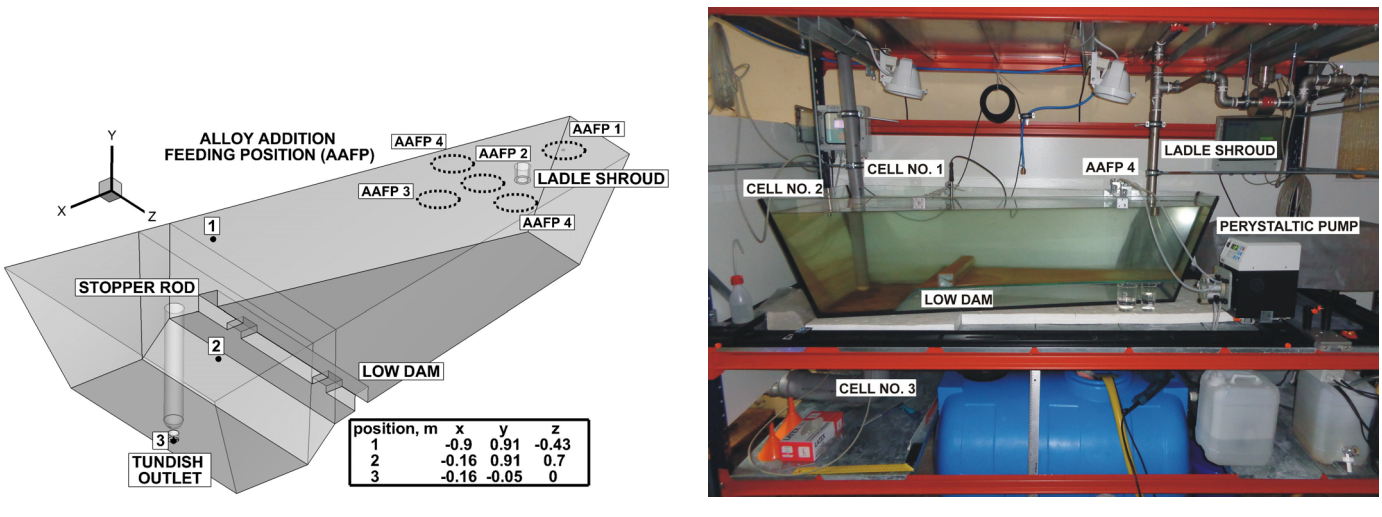

a) b)

Fig. 1. One strand tundish: a) virtual model with considered AAFP and positions of measurement points, b) physical model with AAFP no. 4 and positions of conductometric cells

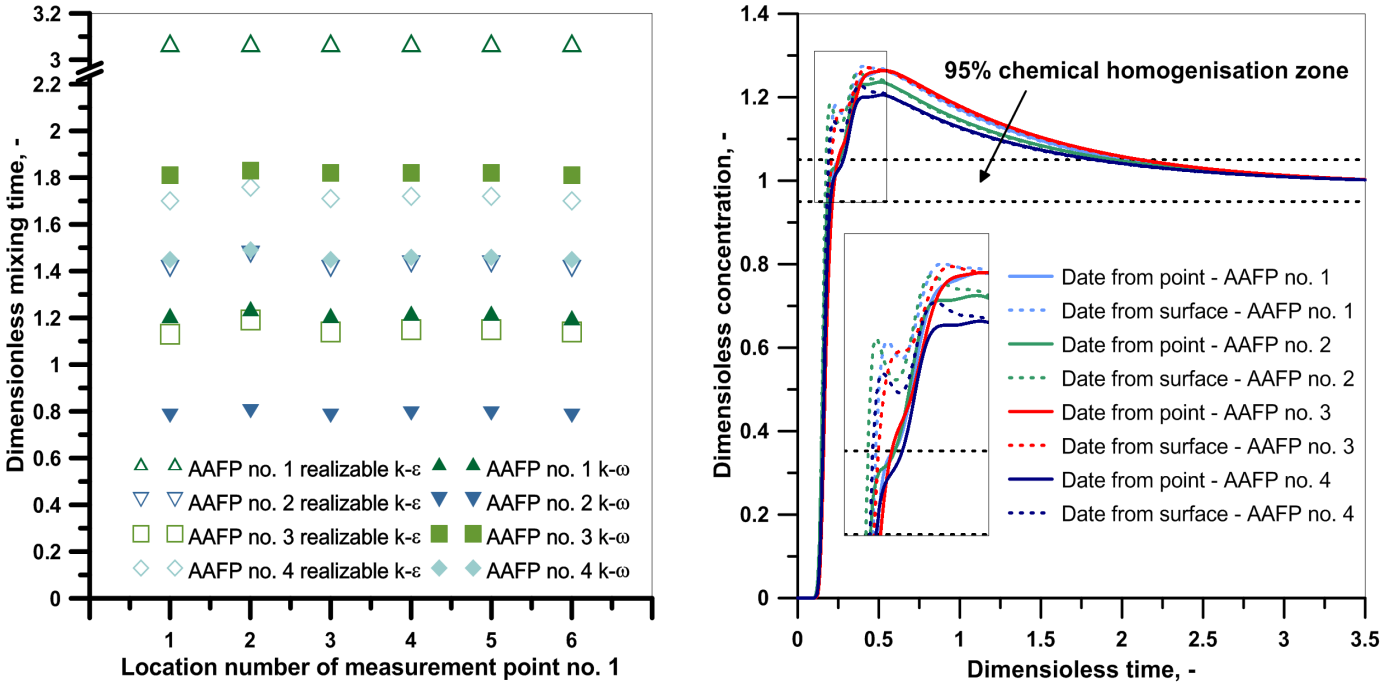

Fig. 2. Mixing time for alloy addition: a) different location of measurement point no. 2 and turbulence model, b) different type of alloy addition monitoring

were tested. Obviously, in individual tundish regions, the chemical homogenisation process will proceed differently. Whereas, the test carried out concerned a slight shift of the base point by 0.05 m in 6 directions. Location no. 1 was the base position as described by the coordinates shown in Figure 1a. Location no. 2, on the other hand, represented the shift of the base point by 0.05 m downwards. Positions no. 3 and no. 4 correspond to the shift of the base point, respectively, towards the stopper rod zone and towards the tundish pouring zone. While in positions no. 5 and no. 6, the base point was shifted, respectively, towards the longitudinal axis and towards the side wall of the tundish. Therefore the recording of alloy addition behaviour in the liquid steel volume is punctual in character. The aim of the simulations was to determine the specific space, in which obtained results were similar. Determining this space was important for the laboratory experiments done (physical simulator) in which, the level of the water underwent periodical slight fluctuations and position of the conductometric sensor was fixed. By contrast, at the second preliminary testing stage, the chemical homogenisation process was monitored at the tundish outlet, while taking into account two types of boundary conditions. The change in alloy addition concentration was monitored from either the point or the transverse surface intersecting the tundish outlet cross-section. At the tundish nozzle it is justifiable to monitor the chemical composition of the liquid steel from the entire cross-sectional surface. It is important for proper estimate of alloying process on a macro scale. Figure 2a illustrates the values of dimensionless mixing time recorded in the stopper rod zone for the alloy addition feed locations under consideration and the turbulence models applied. The obtained differences between individual measurement point locations are very subtle, therefore monitoring the chemical homogenisation process in the space under consideration will yield similar mixing time values. It can be seen, however, that in spite of using the identical location of alloy addition introduction to the liquid steel, change in the turbulence model results in different mixing time values. For the realizable k-ε model, greater mixing times were obtained for feed positions no. 1 and no. 4, and smaller for feed positions no. 2 and no. 3, compared to the results for the alloying process obtained with the use of the k-ω model (Fig. 2a). Figure 2b represents mixing curves for the computations using the realizable k-ε model, as recorded at the tundish outlet with the use of the measurement point or plane. The distribution of the curves suggests that the measurement area does not significantly influence the position of the curve at the time of passing to the 95% chemical homogenisation zone. By contrast, significant differences can be seen in the first period of alloy addition dispersion in the liquid steel, where, in the case of monitoring the tracer concentration change from the point, the curve increments smoothly up to a point, at which its characteristic peak forms. Whereas, when recording the curve in the plane, an intermediate peak arises before the main peak, which indicates variation in the chemical composition of the steel being cast across the transverse plane of the nozzle, in spite of its small size (0.07 m). Considering the obtained results, a decision was made that, at the subsequent testing stage, the change in alloy addition concentration would be examined by monitoring the alloy addition in the transverse plane intersecting the tundish outlet. While the final choice of the turbulence model would be possible to be made after completion of the laboratory experiments on the physical simulator.

4. Behavior of alloy in the tundish

The results obtained from the physical and numerical simulations enabled the assessment of the alloy addition behavior in the liquid steel. Figure 3 depicts the results for the time that elapsed from the alloy addition feed starting point until the occurrence of the maximum concentration value peak on the mixing curve recorded at the monitoring points under consideration. Closest to the alloy addition feed zones is measurement point no. 1, and then points no. 2 and no. 3. Therefore, the time of occurrence of the maximum value peak on the mixing curve should steadily grow as the distance to the tundish outlet zone diminishes. Such a distribution was recorded for all alloy addition feed position variants, as well as for both turbulence models. Whereas, for the realizable *k-ε* model, the shortest times of peak occurrence on the curves were obtained for alloy addition variants no. 2 and no. 4, and which amounted to 0.372 and 0.383 dimensionless time (DT), respectively. By contrast, the results obtained for the mixing process using the *k-ω* model showed a smaller difference in time between individual alloy addition feeding positions (no. 2 and no. 3), as well as much shorter times, compared to the results for the realizable *k-ε* model (0.172-0.183 DT). While the

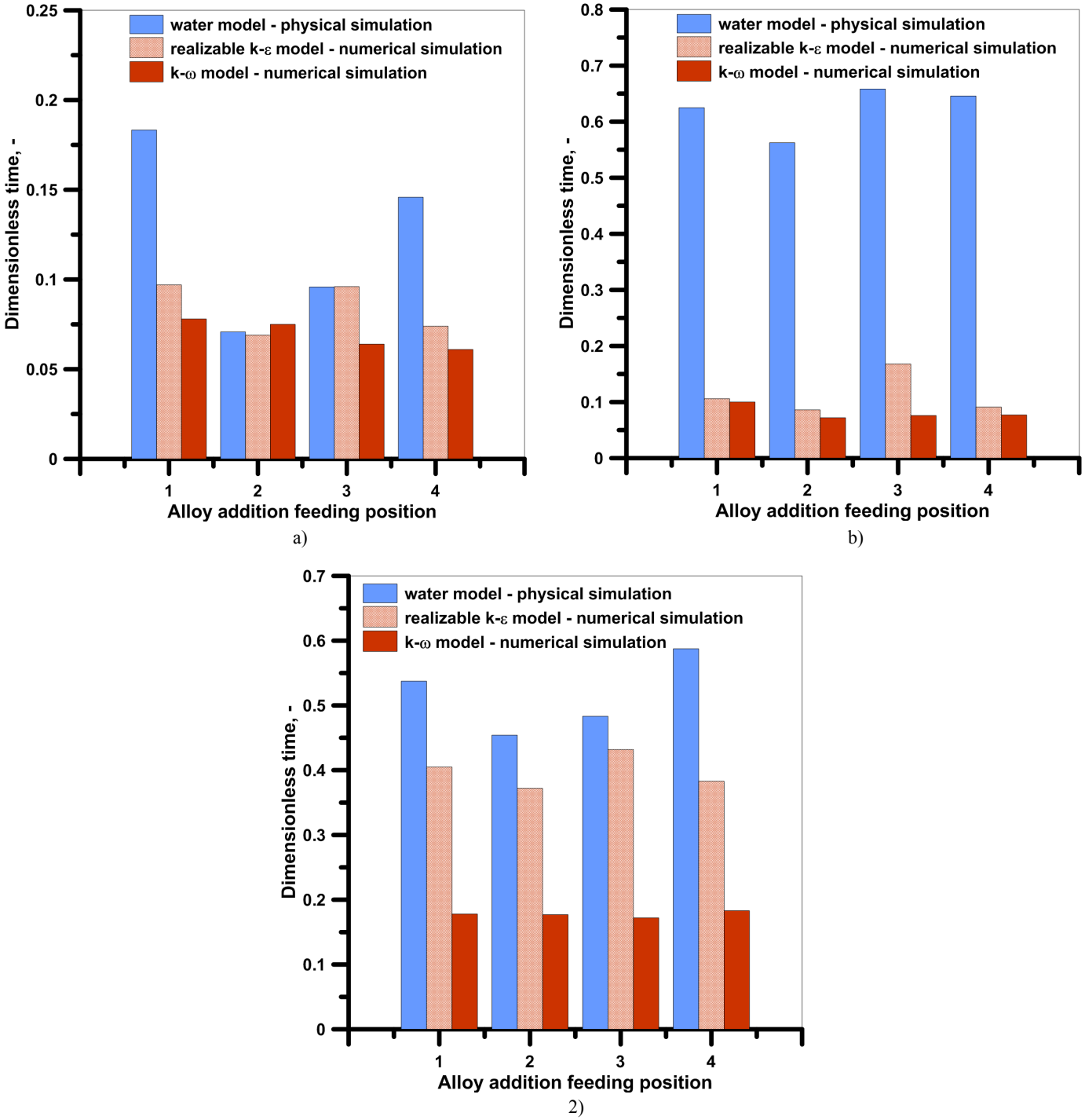

Fig. 3. Apparition time of first peak on mixing curves: a) measurement point no. 1, b) measurement point no. 2, c) tundish outlet

laboratory experiment did not confirm the alloy addition behavior that was recorded in computer simulations. That was because the times of peak occurrence on the curve are greater for the stopper rod zone than for the tundish outlet. This suggest a different alloy addition distribution in the physical model and a distortion of the expected picture of alloy addition behavior. This might be caused by periodical modifications of the hydrodynamic patterns occurring in the water and formed by local streams [21]. This process influences also the kinetic energy dissipation rate, which is definitely unsteady in character. In this connection, the results obtained from both turbulence models in computer simulations are different on the micro-mixing level.

In order to make the ultimate assessment of the usefulness of the tested turbulence models in computer simulations, laboratory experiments were performed, during which mixing curves were recorded at the tundish outlet. Laboratory experiments for individual alloy addition feed location variants were repeated several times to finally select the 6 most similar to one another in value. It can be seen from the results in Figure 4 that the laboratory experiments fairly well correlate with the computer simulation results for the realizable *k-ε* model, especially for the point, at which the curves come within the 95% chemical homogenization region. By contrast, the experimental points deviate from the curve recorded in computer simulations using

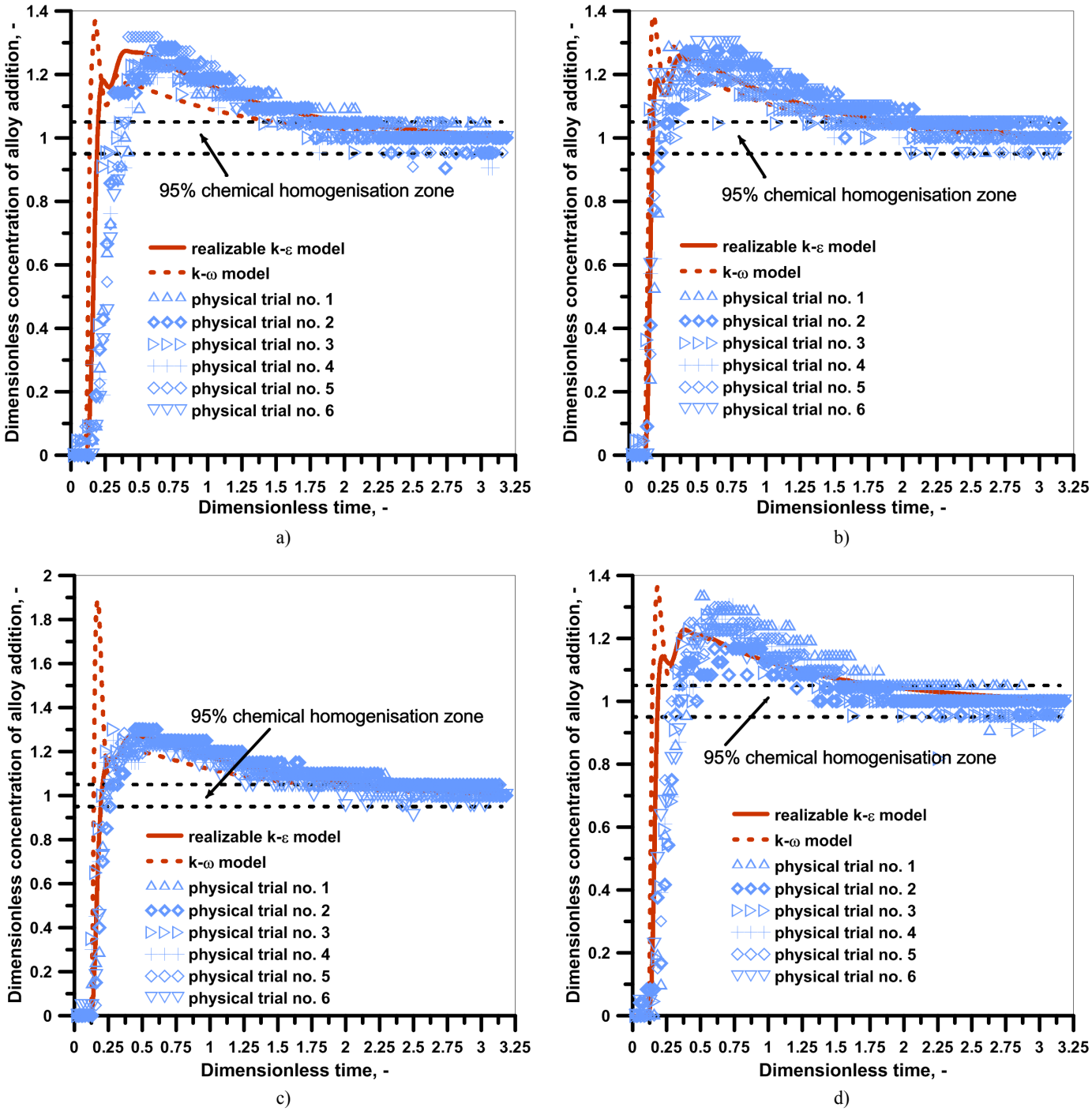

Fig. 4. Mixing curves of alloy addition: a) AAFP no. 1, b) AAFP no. 2, c) AAFP no. 3, d) AAFP no. 4

the *k-ω* model, especially at the initial stage of alloy addition dispersion within the liquid steel volume.

Based on the recorded mixing curves, the mixing time necessary for attaining 95% chemical homogenization was calculated (Fig. 5). The smallest differences in mixing time between the experiment and the computation were obtained for the realizable *k-ε* turbulence model. In addition, the computer simulation results for the realizable *k-ε* model exhibited the same regularity concerning the effect of the change in alloy addition feed position on the mixing time. Indeed, the most favorable alloy addition mixing conditions were obtained for the variant in which the alloy addition was introduced simultaneously in two locations situated at the tundish side walls (AAFP no. 4). By contrast, the worst in terms of chemical homogenization was variant no. 3 of AAFP. For the *k-ω* model, a linear increase in mixing time was obtained for successive variants of alloy addition feed location. Whereas, the most favorable variant was variant no. 1 of AAFP. Therefore, it has been concluded that the realizable *k-ε* model better reflects the hydrodynamic conditions forming in the investigated facility, whereby the chemical homogenization process itself is also be more fit for the real conditions. It has also been demonstrated that, in spite of the deficiencies in predicting the mixing process on the micro level by both turbulence models, the macro mixing picture is clearly acceptable.

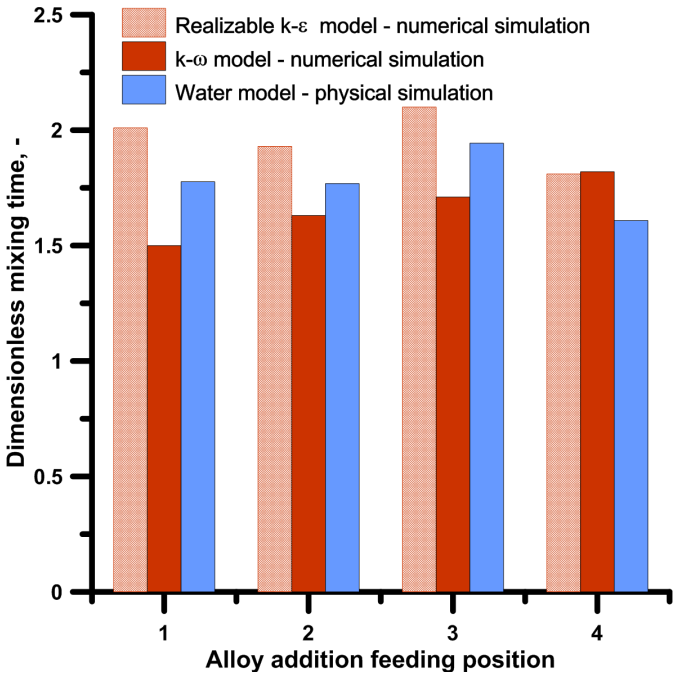

Fig. 5. Dimensionless mixing time of alloy addition – results from mathematical and physical simulations

5. Behavior of liquid steel in the tundish

This section reports liquid steel flow results obtained from computer simulations using the realizable *k-ε* model. Differences in mixing time were obtained for the same tundish equipment variant, but for different locations of feeding the alloy addition. Therefore, change in alloy addition feed position makes other liquid steel streams responsible for the process of the initiation and then mixing of the alloy addition with the liquid steel. Figure 6 shows liquid steel flow maps recorded in horizontal planes arranged in parallel to the tundish bottom. The planes were generated at four depths, namely 0.002, 0.22, 0.44 and 0.66 m, as measured from the liquid steel free surface. At the initial moment, the alloy addition and liquid steel mixing process is determined by the streams located immediately at the free surface. In the case of alloy addition feeding position no. 1 it can be noticed that the liquid steel streams flow in from the tundish side walls to the centre and then they flow on towards the pouring zone, whereby the alloy addition is additionally stimulated by the tundish feeding streams. In the case of AAFP no. 2 and no. 4, on the other hand, the steel streams push the alloy addition along the longitudinal tundish axis, that is towards the central tundish part. In AAFP no. 3, strong circulation exists that hampers the effective spread of the alloy addition within the liquid steel, which is reflected by the longest mixing time noted for this particular variant. In general, the liquid steel streams located immediately at the free surface flow from the tundish side walls towards the tundish centre. It is only from about the mid-tundish length that streams bound for the stopper rod zone arise immediately at the side walls, which flow on towards the tundish front wall. The deeper, the more local recirculation regions occur within the liquid steel. Especially as already 0.22 m below the steel free surface, reverse streams form, particularly in the central tundish part. At the level of 0.48 m from the tundish bottom, reverse streams flowing in from the stopper rod zone effectively prevent the inflow of the tundish feeding streams from the steelmaking ladle. As a result, four large recirculation regions form. Immediately at the bottom, feeding streams can be seen, which flow up to the dam and then flow around it immediately at its side walls. In the central tundish zone this is impossible due to the occurrence of reverse streams flowing in from the stopper rod zone. The hydrodynamic pattern illustrated in Figure 6 is so much varying that the change in the alloy addition feed location alone will influence the chemical homogenization process. The hydrodynamic pattern occurring in alloy addition variant no. 4 is the most advantageous because of the streams that effectively spread the alloy addition within the liquid steel.

6. Summary

Based on the computer simulations and water model trials carried out, it has been found that:

- For considered one strand tundish dynamically variations of liquid steel rotational motion zones were observed. In the mid-depth of melt, liquid steel circulation zones are characterized by the most horizontal area.
- The distribution of points describing the alloy addition mixing curves, as obtained from the laboratory experiments, is similar to the mixing curves obtained from computer simulations in which the realizable *k-ε* model was used.

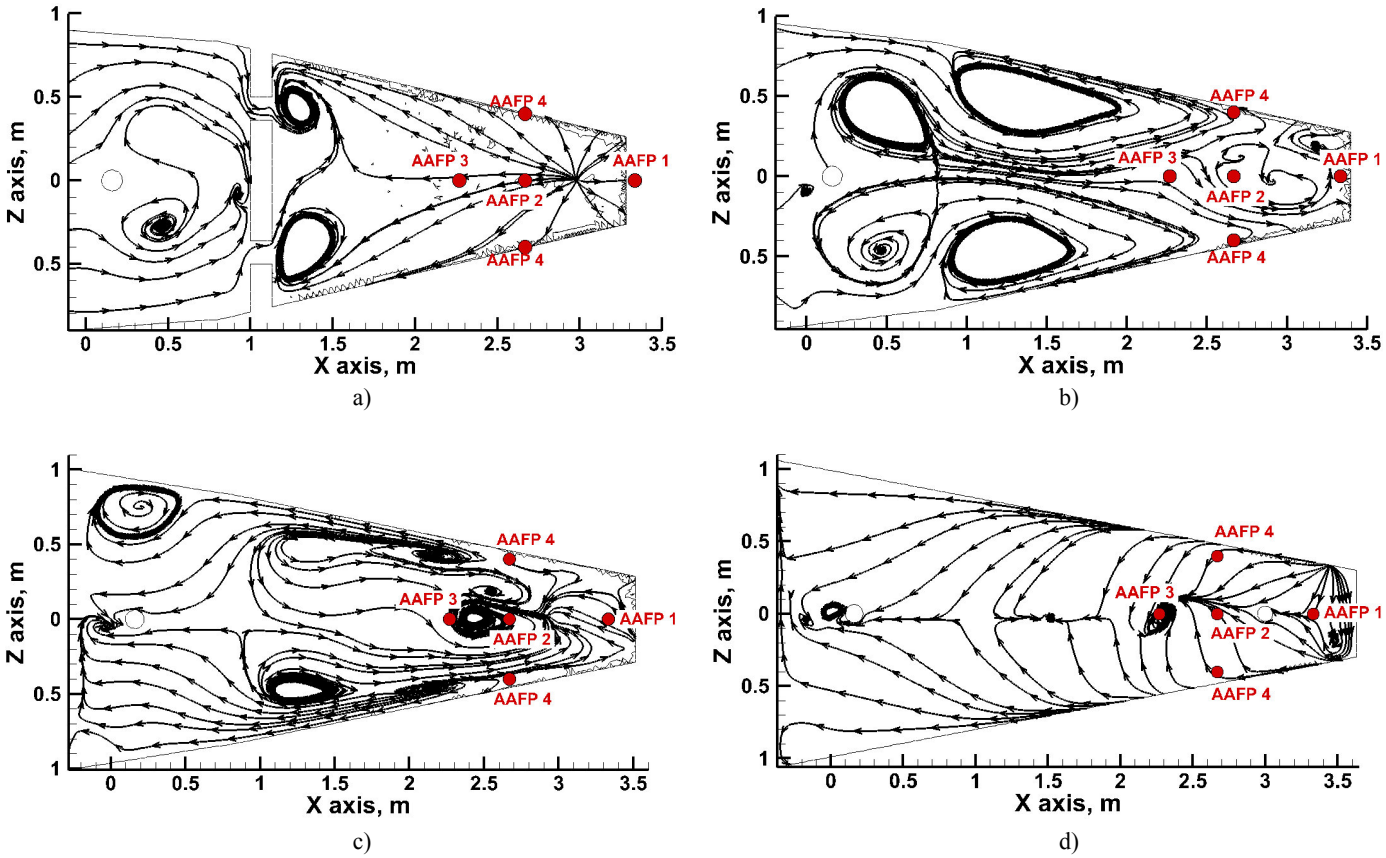

Fig. 6. Liquid steel paths in the tundish: a) level 0.26 m, b) level 0.48 m, c) level 0.70 m, d) level 0.918 m

- In computer simulations using the realizable k-ε model, an identical trend for the effect of the alloy addition feed position on the alloy addition and steel mixing time was obtained.
- The shortest mixing time of alloy addition with liquid steel, while providing 95% chemical homogenization, was obtained for alloy addition feeding position no. 4.

Acknowledgements

This scientific work has been financed from the resources of National Science Centre, Poland in the years 2017-2019 as Research Project No. 2016/23/B/ST8/01135

REFERENCES

[1] P.D. Lee, P.E. Ramirez-Lopez, K.C. Mills, B. Santillana, Ironmak. Steelmak. **39**, 244-253 (2012).
[2] J. Falkus, K. Miłkowska-Piszczek, Mater. Technol. **49**, 903-912 (2015).
[3] L. Ren, L. Zhang, Q. Wang, Metall. Res. Technol. **115**, 102 (2018).
[4] M.M. Salazar-Campoy, R.D. Morales, A. Nájera-Bastida, I. Calderón-Ramos, V. Cedillo-Hernández, J.C. Delgado-Pureco, Metall. Mater. Trans. B **49**, 812-830 (2018).
[5] T. Merder, M. Warzecha, Metall. Mater. Trans. B **43**, 856-868 (2012).
[6] T. Merder, J. Pieprzyca, Steel Res. Int. **83**, 1029-1038 (2012).
[7] J. Falkus, J. Lamut, Arch. Metall. Mater. **50**, 709-718 (2005).
[8] C. Chen, L.T.I. Jonsson, A. Tilliander, G. Cheng, P.G. Jönsson, Metall. Mater. Trans. B **46**, 169-190 (2015).
[9] D. Chen, X. Xie, M. Long, M. Zhang, L. Zhang, Q. Liao, Metall. Mater. Trans. B **45,** 392-398 (2014).
[10] Q. Yue, C.B. Zhang, X.H. Pei, Ironmak. Steelmak. **44**, 227-236 (2017).
[11] K. Morales-Higa, R.I.L. Guthrie, M. Isac, R.D. Morales, Metall. Mater. Trans. B **44**, 63-79 (2013).
[12] A. Ramos-Banderas, R.D. Morales, L. García-Demedices, M. Díaz-Cruz, ISIJ Int. 43, 653-662 (2003).
[13] S. Chatterjee, D. Li, K. Chattopadhyay, Metall. Mater. Trans. B **49**, 756-766 (2018).
[14] A. Mabentsela, G. Akdogan, S. Bradshaw, J. S. Afr. Inst. Min. Metall. **117**, 469-483 (2017).
[15] L. Zhang, Steel Res. Int. **76**, 784-796 (2005).
[16] M. Warzecha, T. Merder, P. Warzecha, G. Stradomski, ISIJ Int. **53**, 1983-1992 (2013).
[17] A. Cwudziński, Ironmak. Steelmak. **42**, 373-381 (2015).
[18] A. Cwudziński, Metall. Res. Technol. **112**, 308 (2015).
[19] A. Cwudziński, Steel Res. Int. **81**, 123-131 (2010).
[20] A. Cwudziński, Ironmak. Steelmak. **42**, 132-138 (2015).
[21] A. Cwudziński, Steel Res. Int. **85**, 902-917 (2014).